*Technical Report*

# Improvement of Sensitivity and Resolution of Solid State NMR for Quadrupolar Nuclei

Takafumi TAKAHASHI*        Koji KANEHASHI

## Abstract

*In NMR measurements of quadrupolar nuclei, the spectral analysis has troublesome because of large line width of NMR peak that is caused by second-order quadrupolar interaction. As a result of application of MQMAS to structural analyses of coal and clay minerals, the substantial increase of spectral resolution archived has enabled us to elucidate their fine chemical structures. On the other hand, we have addressed establishment of STMAS method, because sensitivity of MQMAS is too low to perform the analysis of trace amounts of elements. A new developed NMR probe with feature of very precise adjustment of magic angle, which is critical in STMAS, has attained sensitivity enhancement of up to approximately 5 times compared to MQMAS. Since sensitivity and resolution of these methods are furthermore improved by the combination with high magnetic field strength, their application are promised for low-sensitive nuclei and low-level elements, which have been regarded as quite difficult to measure.*

## 1. Introduction

Slag and coal ash are among inorganic oxides made up of multiple components. In order to propose effective utilization or new methods of treating these materials, it is essential to clarify their chemical structures on a microscopic level. Since such inorganic materials have a complicated structure, solid-state nuclear magnetic resonance (NMR) that permits information about element-specific microstructures to be obtained is an effective tool for analyzing their structures. On the other hand, $^{27}Al$, $^{17}O$ and, $^{11}B$, which are the principal nuclides making up these inorganic materials, have a nuclear spin ($I$) of 7/2, 5/2, and 3/2, respectively. Because of this, unlike $^{1}H$ and $^{13}C$ ($I = 1/2$), these nuclides cause nuclear charges to become spherically asymmetrical and distortions to occur.[1] As a result, owing to the perturbation of the second-order nuclear quadrupolar interaction on the Zeeman splitting, the peak observed deviates from the true chemical shift and the peak line increases in width or splits, making it difficult to carry out detailed structural analysis.

Accordingly, we focused our attention on the multiple-quantum magic-angle spinning (MQMAS) method that enables averaging of the second-order nuclear quadrupolar interaction. By applying MQMAS in a strong magnetic field, we obtained high-resolution, solid-state NMR spectra of quadrupolar nuclei and elucidated the fine structures of the inorganic components in slag and coal ash. However, we were unable to clarify the chemical structures of trace elements in these inorganic materials because the MQMAS technique, which utilizes multiple-quantum transition, has extremely low sensitivity.

Therefore, with the aim of achieving higher sensitivity while maintaining a high resolution comparable to that of MQMAS, we sought to establish the satellite-transition magic-angle spinning (STMAS) method. Obtaining STMAS spectra requires precise adjustment of the magic angle and high stability of the specimen rotational frequency. By developing a new probe possessed of these re-

* Senior Researcher, Ph.D., Materials Characterization Research Lab., Advanced Technology Research Laboratories
  20-1, Shintomi, Futtsu, Chiba

quirements, we achieved an analytical sensitivity much higher than that of MQMAS. As a result, it has become possible to analyze even the structures of trace elements using STMAS.

## 2. Main Subjects

### 2.1 Averaging of the second-order nuclear quadrupolar interaction

In NMR analysis of quadrupolar nuclei with basically a half-integer spin, central transition is observed. The reason for this is shown in **Fig. 1**, where the central transition is unaffected by the quadrupolar interaction within the range of first-order perturbation. However, when the specimen is a solid, such as a powder, a second-order shift occurs, causing the line width to increase. Assuming that the specimen is rotated at angle $\beta$ against a static magnetic field, the central peak, $\nu$, produced by the second-order perturbation can generally be expressed by the following equation.

$$\nu = \nu_Q^2 / \nu_L \left[ A_0 + A_2(\theta, \psi) P_2(\cos\beta) + A_4(\theta, \psi) P_4(\cos\beta) \right] \quad (1)$$

In the above equation, $\nu_Q$, $\nu_L$, $A_o$, $A_2(\theta, \psi)$, and $A_4(\theta, \psi)$ denote the quadrupolar interaction frequency, Zeeman interaction frequency, isotropic term, and functions ($A_2$, $A_4$) that are dependent on the direction of the specimen tube rotational axis and on the orientation of the microcrystal, respectively.

The $P_2$ and $P_4$ terms are second-order and fourth-order terms in the Legendre function. From **Fig. 2**, the magic angle is angle $\beta$ at which $P_2(\cos\beta) = 0$. Therefore, the $A_2$ term can be eliminated by MAS, whereas the $A_4$ term is retained. Thus, the increase in line width ascribable to the second-order perturbation cannot be completely eliminated even by MAS. Therefore, in order to achieve high-resolution NMR analysis of quadrupolar nuclei, it is essential to eliminate the $A_4$ term.

From Fig. 2, each of the $P_2$ and $P_4$ terms that correspond to the second- and fourth-order terms in the Legendre function can be eliminated by using a different angle, $\beta$. The idea behind DOR (double rotation) is that the specimen is rotated at two different angles simultaneously to eliminate the two terms.[2] Concretely expressed, the external rotation angle is $54.7°$ and the internal rotation angle is $70.1°$ (or $30.6°$), and the rotational ratio between them needs to be 5 or more.

Dynamic angle spinning (DAS) is an approach whereby the axes of rotation are moved to impart angular dependence to $\beta$ and eliminate the $A_2$ and $A_4$ terms simultaneously as values integrated over time in which transverse magnetization is propelled.[3] Thus, if $\beta$ consists of only discontinuous angles $\beta_1$ and $\beta_2$ and if the transverse magnetization showing these two angles lasts only for the time at

which these two angles are equal, the $A_2$ and $A_4$ terms are eliminated when angle $\beta_1$ ($37.38°$) and angle $\beta_2$ ($79.18°$), which make $P_2$ ($\cos\beta_1$) + $P_2$ ($\cos\beta_2$) = 0 and $P_4$ ($\cos\beta_1$) + $P_4$ ($\cos\beta_2$) = 0, are chosen. In the experiment, with the specimen kept rotating about the axis of rotation that forms angle $\beta_1$, transverse magnetization is time-propelled for time $\tau_1$. Next, angle $\beta_1$ is switched to angle $\beta_2$. During the switching time, it is irradiated with a $90°$ pulse to keep the magnetization in the direction of the static magnetic field.

After that, it is again irradiated with a $90°$ pulse to propel transverse magnetization during rotation in the $\beta_2$ direction. Then, $\tau_1$ later, the decay caused by chemical shift and quadrupolar anisotropies is recovered as an echo. Sampling the echo amplitude for various development times $t_1 = 2\tau_1$, it is time-propelled by the sum of the isotropic averages of the two interactions. This echo is called an isotropic echo signal. By subjecting it to a Fourier transform, it is possible to obtain a high-resolution spectrum. In addition, by recording the decay from the vertex of the echo as a function of ($t_1$, $t_2$) and subjecting it to a two-dimensional Fourier transform, it is possible to obtain a two-dimensional spectrum in which the isotropic average and anisotropy appear on the frequency $\omega_1$ and $\omega_2$ axes, respectively, as in the case of MQMAS described later.

MQMAS is an approach whereby the coherence order is varied until an isotropic echo is obtained.[4] It uses a powerful radio frequency (rf) to excite multiple-quantum coherences and selects a specific multiple-quantum coherence by means of phase cycling (e.g., 1 × 6 × 4 = 24 times). In the sequence using the z-filter shown in
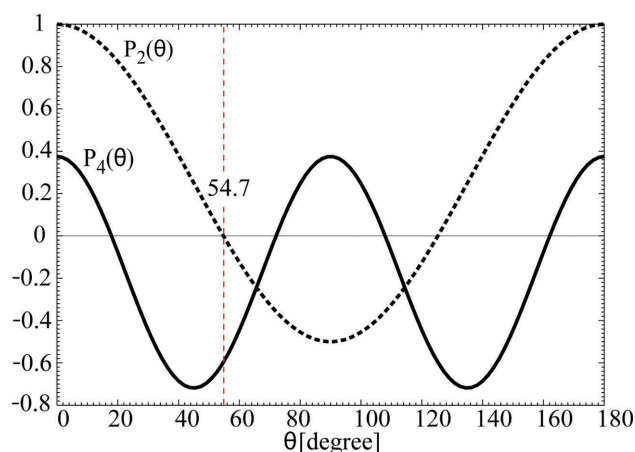
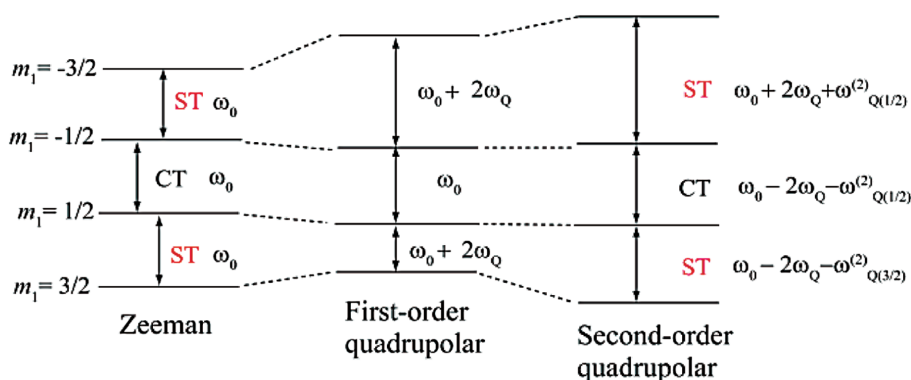**Fig. 2 Angular dependency of $P_2(\cos\beta)$ and $P_4(\cos\beta)$ terms in Legendre function**

**Fig. 1 Energy level for a nucleus with nuclear spin $I = 3/2$ in a static magnetic field**

**Fig. 3**,[5)] the coherent paths are made symmetrical to eliminate the variance components.

The principle on which MQMAS is based is similar to that of the reconstruction of an isotropic term in DAS. The largest difference is that MQMAS uses multiple-quantum coherences, not angles. The second-order perturbation term for the central transition ($-m \leftrightarrow +m$) in multiple-quantum transitions can be expressed by the following equation, which is similar in form to Equation 1 for a single-quantum transition.

$$\nu_{-m \leftrightarrow +m} = \nu_Q^2 / \nu_L \left[ A_0 C_0^I(m) + A_2(\theta, \psi) C_2^I(m) P_2(\cos \beta) \right.$$
$$\left. + A_4(\theta, \psi) C_2^I(m) P_2(\cos \beta) \right] \quad (2)$$

The above equation is characteristic in that it contains term $C_0^I$ ($m$) with respect to the coherence order. At the magic angle ($P_2(\cos \beta) = 0$), magnetization with coherence order $m$ is developed for $t_1$ and the coherence is then moved to a single quantum. Then, the condition under which an isotropic echo signal can be obtained after time $t_2$ is expressed by the following equation.

$$t_2 = \left[ C_4^I(m) / C_4^I(1/2) \right] t_1 \quad (3)$$

In the above equation, $C_4^I(m)$ is a value determined by the nuclear spin and coherence order.

The greatest merit of the MQMAS technique is that, unlike the DOR or DAS technique, it permits use of an ordinary MAS probe for measurement. In addition, since it can be used in combination with any of several other sequences, such as CP (cross polarization)
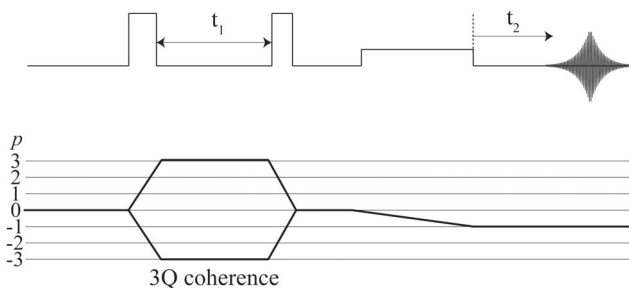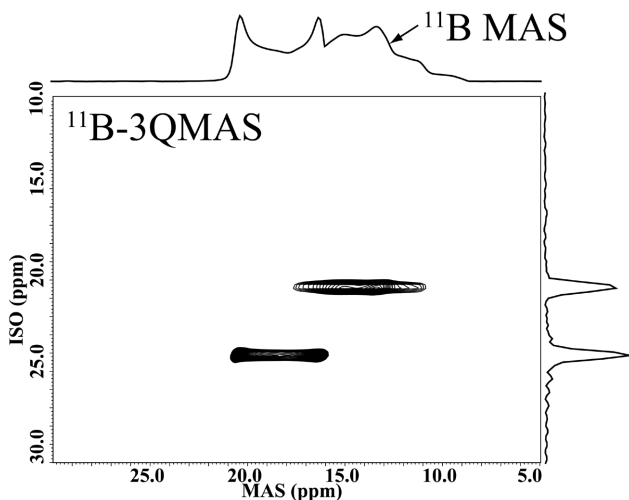
or HETCOR (heteronuclear correlation), it permits information to be obtained about the distance between different nuclides, etc.

An example showing the usefulness of MQMAS spectra is given in **Fig. 4**. In the one-dimensional MAS spectrum, only an asymmetric peak split is observed. On the other hand, the MQMAS spectrum in which the second-order nuclear quadrupolar interactions have been averaged clearly shows two peaks, indicating the presence of two boron (B) sites that differ in their chemical environments.

**2.2 Structural analysis of raw materials in the steelmaking process using MQMAS**

We applied MQMAS to the analysis of the structures of more practical materials. **Fig. 5** shows $^{27}$Al NMR spectra of Coal **a** obtained with a static magnetic field strength of 7.0 *T*. In the MAS spectrum (Fig. 5 (a)), a peak of $^{[6]}$Al and a peak of $^{[4]}$Al were observed. Concerning the $^{[6]}$Al peak in particular, it had broadened asymmetrically. It was uncertain whether this was due to the presence of two or more different minerals or the second-order nuclear quadrupolar interaction. However, since the 3QMAS spectrum (Fig. 5 (c)) clearly shows more than two peaks, it was found that Coal **a** contained two or more different minerals. By comparing the peak positions between this two-dimensional spectrum and the two-dimensional spectra of standard mineral samples, it is possible to identify the types of minerals contained in Coal a. As mentioned earlier, MQMAS can easily be used in combination with any of several other sequences. Therefore, we applied $^1$H → $^{27}$Al CP/MQMAS to Coal **a**. The result is shown in Fig. 5 (b).

In this method, the magnetization of $^1$H nuclei is first transferred to $^{27}$Al nuclei, and MQMAS is then applied to obtain a high-resolution $^{27}$Al NMR spectrum. Therefore, it is possible to selectively detect only the peak for Al that is present in the neighborhood of H. Focusing on $^{[6]}$Al, peaks (1) - (3) were observed in the MQMAS
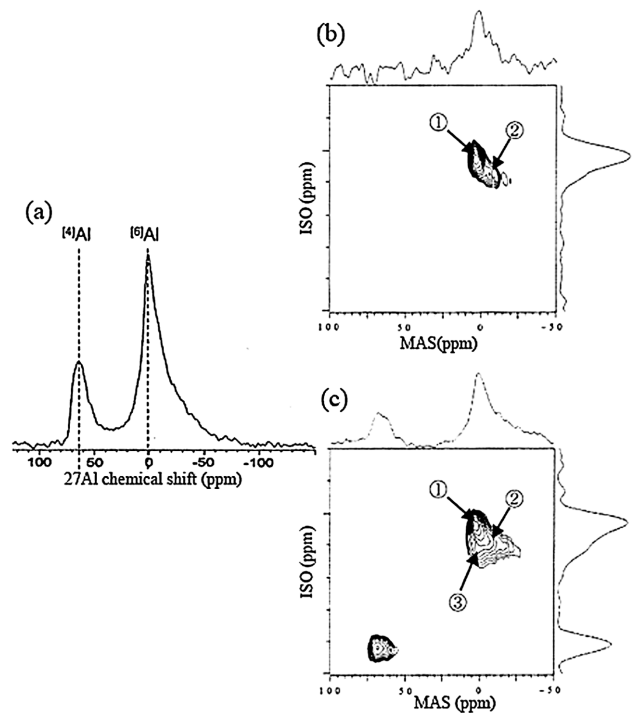


**Fig. 3  3QMAS pulse sequence with z-filer**



**Fig. 4   Comparison of $^{11}$B-MAS and -3QMAS spectra of aboron compound**



**Fig. 5   $^{27}$Al-MAS spectra of natural Coal a**
(a) $^{27}$Al-MAS spectrum at static magnetic field of 7.0T, (b) $^{27}$Al → $^1$H CP/MQMAS spectrum and (c), $^{27}$Al-3QMAS spectrum

spectrum, while only peaks (1) and (2) were selectively observed in the CP/MQMAS spectrum. On the basis of these observation results, we determined that (1) and (2) were clay minerals, such as kaolin, having Al-OH bonds and that (3) was an alumina-based oxide devoid of Al-OH bonds. For nuclides whose spin is 5/2 or more, a higher resolution can be achieved by MQMAS spectrum measurement using higher-order coherence. For example, when the spin ($I$) is 3/2, only 3QMAS measurement is applicable, whereas when $I = 5/2$, 5QMAS measurement can be applied as well as 3QMAS.

Generally, when higher-order coherence is used, the resolution is expected to improve. At the same time, however, the sensitivity deteriorates markedly. Because of this, the number of nuclides that can be measured by 5QMAS is considerably limited. It is known that in the clay mineral montmorillonite, the distribution of vacant sites changes according to the configuration of hydroxyl groups coordinated to [6]Al and that the change influences the physical properties of the clay mineral.[6, 7] Therefore, we attempted to estimate the configuration of hydroxyl groups from the local structure of Al. **Fig. 6** shows the $^{27}$Al-3QMAS and $^{27}$Al-5QMAS spectra of the coordination number 6 region in montmorillonite clay. Multiple Al sites that cannot be identified by 3QMAS spectrum measurement were found for the first time by applying 5QMAS. As a result, it was found that at sites in an octahedral layer where ions are missing, the hydroxyl group shows *cis* configuration.

As has been described above, in solid-state NMR of quadrupolar nuclei, MQMAS spectra often have much higher peak resolution than one-dimensional MAS spectra since the second-order nuclear quadrupolar interactions are averaged. This effect is especially conspicuous with complex materials with a large nuclear quadrupolar coupling constant. On the other hand, because of inefficient excitation of multiple-quantum transition and inefficient conversion into a single quantum, MQMAS suffers from extremely low sensitivity of measurement.

### 2.3 Principles of STMAS

The concept of STMAS is to compensate for the low sensitivity of measurement with MQMAS by substituting the correlation between satellite transition ST (e.g., –3/2 ↔ –1/2) and central transition (–1/2 ↔ 1/2) for the multiple-quantum transition used by MQMAS.

Following the examples given earlier, the excitation of a satellite signal can be expressed as follows.

$$\left\langle v_{1/2 \leftrightarrow 3/2} \right\rangle = \frac{1}{v_L}\left[ B_0\left(\eta\right) + A_2\left(\theta, \phi, \eta\right)B_0\left(I\right)P_2\left(\cos\beta\right) \right.$$
$$\left. + A_4\left(\theta, \phi, \eta\right)B_0^4\left(I\right)P_4\left(\cos\beta\right) \right]\left( \frac{3}{2I\left(I-1\right)}C_Q \right)^2 \quad (4)$$

In the above equation, $\eta$, $\phi$, and $C_Q$ denote the asymmetry parameter, Eulerian angular component, and quadrupolar coupling constant, respectively. STMAS is the same as MQMAS in the sense that, although the coefficient is different, the new term, B, is included to provide a new degree of freedom. As shown in Fig. 1, unlike central transition, satellite transition is subject to first-order perturbation. Therefore, in the STMAS measurement, the most important point is to completely average the first-order nuclear quadrupolar interactions. Specifically, it is essential to precisely adjust the magic angle (to 54.736° ± 0.003°) and completely synchronize the sampling interval in the $t_1$ direction with the specimen rotational speed.

Therefore, we developed a new probe for STMAS that features a mechanism capable of holding the required magic angle for prolonged periods. Also concerning the specimen rotational speed, we succeeded in controlling the fluctuation to within ± 0.002 kHz against 20 kHz. Thus, we have been able to solve the technical problems involved in STMAS.

### 2.4 Comparison of sensitivity and resolution between STMAS and MQMAS

Under these conditions, using kaolin ($Al_2Si_2O_5(OH)_4$, $C_Q$ = 3.6 MHz) and glass (43.1CaO-12.5$Al_2O_3$-44.4$SiO_2$, $C_Q$ = 7.2 MHz), we compared the sensitivity and resolution between STMAS and MQMAS. We measured S/N ratios and half-widths by using 3QMAS and 3Q-SPAM (soft-pulse added mixing) as the pulse sequences for MQMAS measurement and DQF, DQ, and DQF-SPAM as those for STMAS measurement. **Fig. 7** shows the dependence on the rf strength of the S/N obtained by each of the pulse sequences. It can be seen that obtaining a good S/N by MQMAS requires as strong an rf magnetic field as possible. It should be noted, however, that the effect of increasing the rf strength on improving S/N is saturated when the frequency is 90 kHz or higher. It should also be noted that the sensitivity improvement effect shown by STMAS for glass is smaller than that for kaolin. For example, at the maximum rf strength, the sensitivity improvement effect shown by STMAS for kaolin was a maximum of 4.5 times greater than that shown by 3Qz (3QMAS with a z-filter), whereas the sensitivity improvement effect for glass was a maximum of three times greater. This difference in sensitivity im-
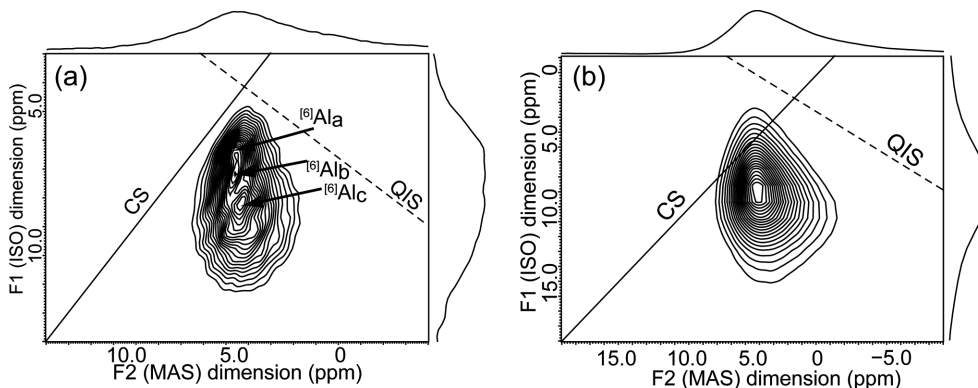


**Fig. 6** $^{27}$Al-MQMAS spectra of Na-montmorillonite
(a) 5QMAS and (b) 3QMAS

provement effect is considered ascribable to the crystallinity of the specimen, rather than the intensity of the quadrupolar interaction. Specifically, in the case of an amorphous material like glass, satellite transition (ST) signals in the form of a sideband appear less readily than in the case of kaolin of higher crystallinity, and hence, the intensity of the ST signal observed is lower. This is estimated to cause the S/N of the STMAS spectra to deteriorate and the sensitivity improvement effect to decrease.

To evaluate the resolution of each of the pulse sequences, we calculated the half-widths from spectra projected onto the $F_1$ axis. Since the half-widths did not show any dependence on rf strength, each of the values obtained for the pulse sequences at the maximum rf strength was assumed to be the half-widths for the appropriate pulse sequence. **Table 1** compares the measured half-widths of kaolin and glass with the homogeneous broadening factor that has already been reported.[8] It can be seen that the half-widths obtained with kaolin nearly coincide with the reported value, but that all the STMAS half-widths obtained with glass are greater than the MQMAS half-widths. Noting that the nuclear quadrupolar interaction at the [4]Al site of glass is conspicuous, it is considered due to the broadening of the STMAS spectra under the influence of higher-order interactions (third-order quadrupolar interaction, intersection term between chemical shift anisotropy, and second-order nuclear quadrupolar interaction), which do not influence the symmetrical transition.

However, the effect of using STMAS on the resolution in glass analysis is considered small since glass essentially has a wide structural distribution and the peak itself shows a wide line width. From all these considerations, by adopting STMAS, especially with the DQF-SPAM pulse sequence, it is considered possible to obtain the maximum sensitivity improvement effect while maintaining a reso-

lution comparable to that of MQMAS.

**2.5 Implementation of chemical structure analysis for trace elements by STMAS**

We attempted to analyze the chemical form of a trace amount of boron using the DQF-SPAM pulse sequence. Boron is one of the elements subject to environmental emission regulations that have recently been made more stringent. In promoting the utilization of coal ash, etc., therefore, fixing boron has become a major challenge. From studies conducted in the past,[9] it is estimated that the chemical structure of boron governs the characteristics of its elution. Also from the standpoint of identifying the phase that contributes to boron fixing, a technology to analyze the chemical form of the trace element has been called for.

**Fig. 8** shows [11]B-MAS spectra for a raw coal and a coal ash. In the spectrum for raw coal, three boron sites were distinguished and the nuclear quadrupolar coupling constant ($C_Q$) at each of these sites was as small as 0.9 MHz. Therefore, the boron is identified as tetrahedral boron [4]B. Judging from the region of the chemical shift and the results of a combustion test, only Site a derives from an inorganic borate oxide and the other Sites b and c derive from organic boron (organoboron).[10]

On the other hand, after the raw coal was burned to ash at 1,500 ℃, all the boron sites became [3]B. From the region of its chemical shift, it is assumed that the boron exists in the form of $Ca_2B_2O_5$ and $Ca_3B_2O_6$. In fact, by elemental mapping of the same specimen using secondary ion mass spectrometry (SIMS), it has been found that boron and calcium strongly correlate and coexist in particles of coal ash.[11] This fact supports the above assumption.

As described above, the STMAS technique has made it possible to analyze the chemical structure of trace elements in materials. In
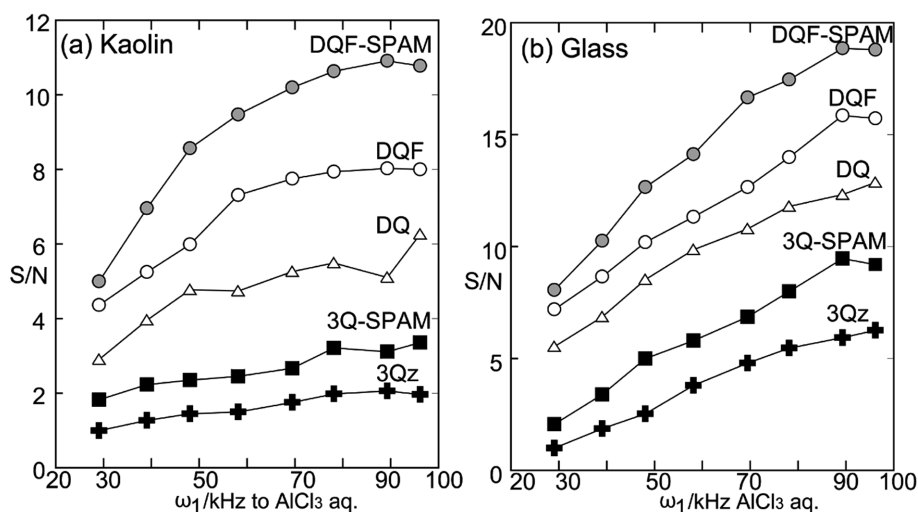


**Fig. 7 Dependence of S/N (signal to noise) ratios on the applied rf field strengths in the observation of (a) kaolin and (b) glass**
**Note that S/N ratio for each pulse sequence is normalized by that for 3Qz**

**Table 1 Comparison of resolution between STMAS and MQMAS based on the full widths at half maximum of NMR spectra projected on ISO axis (Note that each value is normalized by that for 3QMAS)**

|  | DQF-SPAM | DQF | DQ | 3Q-SPAM | 3Qz | 5Qz |
|---|---|---|---|---|---|---|
| Kaolin | 0.96 | 0.96 | 1.31 | 0.87 | 1 | 0.45 |
| Glass | 1.26 | 1.26 | 1.36 | 1.08 | 1 | 0.79 |
| Ref. [*1] | 1 | 1 | 1.77 | 1 | 1 | 0.24 |

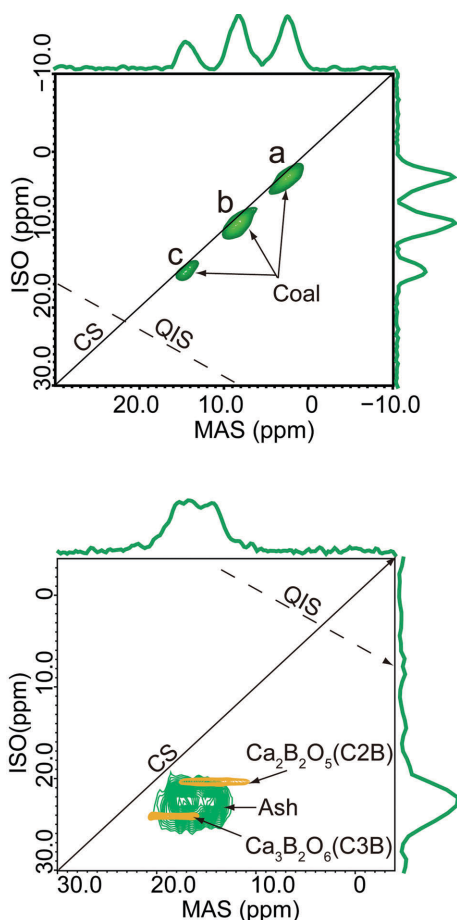[*1] Trebosc et al.[8]: Homogeneous broadening factor

**Fig. 8** ¹¹B-STMAS NMR spectra for (a) raw coal and (b) coal ash Concentration of boron for the raw coal and the coal ash is estimated to be 0.008mass％ and 0.05mass％, respectively.



**Fig. 9** Relationship between static magnetic field strength (in Tesra, *T*) and signal to noise (S/N) ratio for Al sites with various $P_Q$ values





**Fig. 10** ²⁷Al-3QMAS NMR spectra of natural coal (b) acquired at static magnetic fields of (a)7.0*T* and (b)16.4*T*

fact, however, the sensitivity of the STMAS technique depends more or less on the value of $C_Q$, causing the marginal concentration to vary. Specifically, when the $C_Q$ value is in the range 0 to 1 MHz, it is possible to measure boron concentrations down to approximately 0.005 mass% in one week; however, when the $C_Q$ value is 2 MHz or more, it is considered that the measurable boron concentration limit is approximately 0.04 mass%, or 10 times higher.

**2.6 Effectiveness of strong-magnetic-field NMR**

So far, we have discussed the improvement in sensitivity and resolution of spectral measurements through development of such techniques as MQMAS and STMAS. As a matter of fact, the magnetic field in which they are used is an important factor. Therefore, we studied the influence of magnetic field strength.

**Fig. 9** shows the relationship between static magnetic field strength and the S/N ratio obtained from several different Al-containing compounds. In the case of compounds devoid of nuclear quadrupolar interaction ($P_Q = 0$), theoretically, the S/N ratio improves in proportion to the magnetic field strength ($B_o$) raised to the power of 3/2. On the other hand, for compounds subject to nuclear quadrupolar interaction ($P_Q \neq 0$), improvement in the S/N ratio is more than the theoretical value. This is especially conspicuous with compounds subject to stronger quadrupolar interaction. The reason for this phenomenon is considered to be follows. Since the broadening of the peak caused by the second-order perturbation is inversely proportional to the square of resonance frequency on a ppm scale,
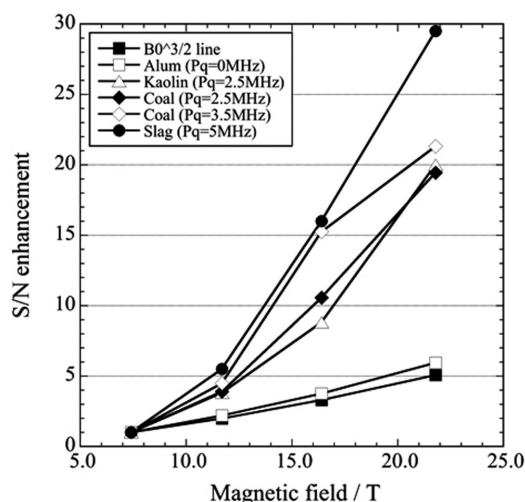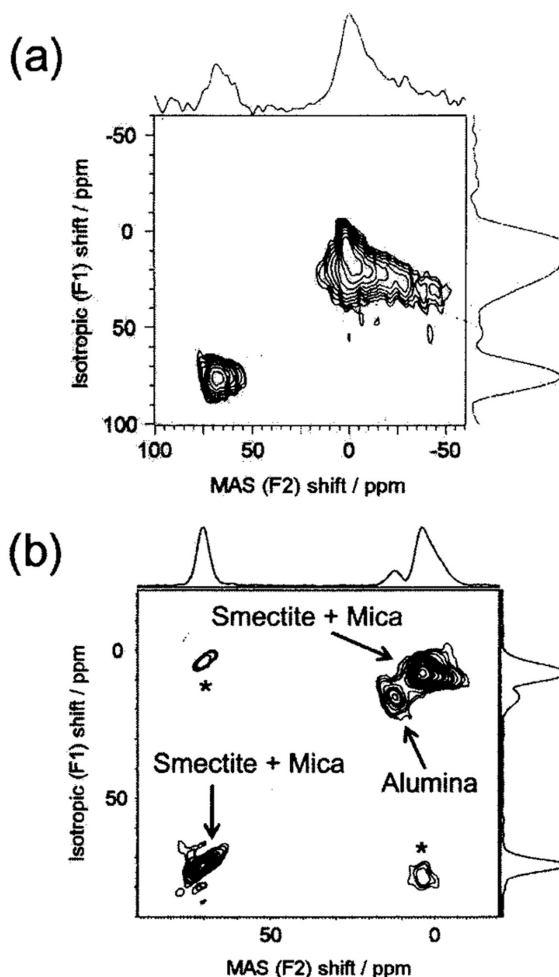
the apparent improvement in the S/N ratio becomes greater when $P_Q$ is larger.

**Fig. 10** shows ²⁷Al 3QMAS spectra for Coal b obtained with varying static magnetic field strengths. An [6]Al peak that could not be

clearly observed at 7.0 $T$ (Fig. 10 (a)) could be clearly confirmed at 16.4 $T$ (Fig. 10 (b)). Thus, we were able to identify the kinds of Al-containing minerals in the coal. In addition, we have found that there is a certain correlation between the Si/Al content and the kinds of Al-containing minerals in coal.[12]

Also with respect to STMAS, it is possible to confirm an improvement in the S/N ratio up to about five times that with MQMAS at the same static magnetic field strength. Under stronger magnetic fields, STMAS offers still more improvement in sensitivity. Concerning the boron contained in coal ash shown in Fig. 8, too, an STMAS spectrum could be obtained for the first time by accumulating the signals of about one week of observation at a static magnetic field strength of 16.4$T$. If MQMAS is used at the same static magnetic field strength, the S/N ratio deteriorates so much that the peak itself cannot be obtained. Therefore, we consider that there is room for improvement of the marginal concentration level for STMAS discussed in the preceding section by applying stronger magnetic fields.

## 3. Conclusion

We attempted to improve the resolution and sensitivity of solid-state NMR by establishing MQMAS and STMAS measurement techniques. Through application of these measurement techniques to the analysis of raw materials for the steelmaking process, we obtained the following knowledge.

(1) The MQMAS technique considerably improves the resolution of spectra as compared with the MAS technique. However, because of its principle of applying multiple-quantum coherence, the MQMAS technique has such low sensitivity that it cannot be used to analyze the fine chemical structures of trace elements.

(2) The STMAS technique has a sensitivity about five times higher than that of the MQMAS technique while maintaining a high spectrum resolution comparable to that of MQMAS. Thus, it allows for the structural analysis of low-concentration elements that is otherwise impossible with conventional techniques. In the future, it is expected that the STMAS technique will be mainly applied to the analysis of the fine chemical structures of low-concentration, low-sensitivity elements.

(3) In MQMAS and STMAS spectrum measurements, as well as in MAS spectrum measurement, it is possible to enhance the sensitivity and resolution by using stronger magnetic fields. In particular, measuring spectra in a strong magnetic field is advantageous for sites where the nuclear quadrupolar interaction is very active.

### References

1) Ueda, K., Ohnuki, A.: Physics of Heavy Electron Systems. First Edition. Shokabo Publishing Co., Tokyo, 1998, p. 361
2) Samson, A. et al.: Mol. Phys. 65, 1013 (1988)
3) Terao, T. et al.: J. Chem. Phys. 85, 3816 (1986)
4) Frydman, L., Harwood, J. S.: J. Am. Chem. Soc. 117, 5367 (1995)
5) Amoureux, J. P. et al.: J. Magn. Reson. A. 123, 116 (1996)
6) Dritis, V. A. et al.: Clays and Clay Minerals. 54, 131 (2006)
7) Takahashi, T. et al.: Clays and Clay Minerals. 56, 525 (2008)
8) Trebosc, J. et al.: Solid State Nucl. Magn. Reson. 31, 1 (2007)
9) Kashiwakura, S. et al.: Fuel. 88, 1245 (2008)
10) Takahashi, T. et al.: Environ. Sci. Tech. in press, 2010
11) Hougaudy, J. et al.: J. Chem. Phys. 64, 3840 (1978)
12) Kanehashi, K.: J. Japan Institute of Energy. 88, 119 (2009)
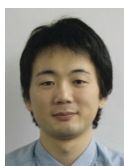
Takafumi TAKAHASHI
Senior Researcher, Ph.D.,
Materials Characterization Research Lab.,
Advanced Technology Research Laboratories
20-1, Shintomi, Futtsu, Chiba

Koji KANEHASHI
Senior Researcher, Ph.D.,
Materials Characterization Research Lab.,
Advanced Technology Research Laboratories